Clinical Neurophysiology 122 (2011) 2016–2024

Contents lists available at ScienceDirect

Clinical Neurophysiology

journal homepage: www.elsevier.com/locate/clinph

Characterization of A phases during the Cyclic Alternating Pattern of sleep

Sara Mariani [a,*], Elena Manfredini [a], Valentina Rosso [b], Martin O. Mendez [c], Anna M. Bianchi [a], Matteo Matteucci [d], Mario G. Terzano [b], Sergio Cerutti [a], Liborio Parrino [b]

[a] Politecnico di Milano, Department of Biomedical Engineering, P.zza Leonardo da Vinci 32, 20133 Milan, Italy
[b] Sleep Disorders Center, Department of Neurology, University of Parma, via Gramsci 14, 43126 Parma, Italy
[c] Universidad Autonoma de San Luis Potosi, Department of Electronics, Salvador Nava S/N, San Luis Potosí, Mexico
[d] Politecnico di Milano, Department of Information Engineering, P.zza Leonardo da Vinci 32, 20133 Milan, Italy

ARTICLE INFO

Article history:
Accepted 28 February 2011
Available online 24 March 2011

Keywords:
EEG
CAP classification
Sleep analysis
Signal processing
Feature selection
Sleep microstructure

HIGHLIGHTS

- A quantitative mathematical characterization of sleep microstructure.
- A study that puts the bases for the implementation of an automatic classifier of the Cyclic Alternating Pattern.
- A novel approach to sleep analysis that gives a mathematical confirmation to the medical literature about CAP.

ABSTRACT

Objective: This study aims to identify, starting from a single EEG trace, quantitative distinctive features characterizing the A phases of the Cyclic Alternating Pattern (CAP).
Methods: The C3-A2 or C4-A1 EEG leads of the night recording of eight healthy adult subjects were used for this analysis. CAP was scored by an expert and the portions relative to NREM were selected. Nine descriptors were computed: *band descriptors* (low delta, high delta, theta, alpha, sigma and beta); *Hjorth activity in the low delta and high delta bands; differential variance of the EEG signal*. The information content of each descriptor in recognizing the A phases was evaluated through the computation of the ROC curves and the statistics sensitivity, specificity and accuracy.
Results: The ROC curves show that all the descriptors have a certain significance in characterizing A phases. The average accuracy obtained by thresholding the descriptors ranges from 59.89 (sigma descriptor) to 72.44 (differential EEG variance).
Conclusions: The results show that it is possible to attribute a significant quantitative value to the information content of the descriptors.
Significance: This study gives a mathematical confirm to the features of CAP generally described qualitatively, and puts the bases for the creation of automatic detection methods.
© 2011 International Federation of Clinical Neurophysiology. Published by Elsevier Ireland Ltd. All rights reserved.

1. Introduction

The electroencephalogram (EEG) provides important and unique information about the sleeping brain. The conventional approach for sleep studies is based on the definition of the sleep *macrostructure*, a stepwise profile that classifies sleep stages according to the prevalent EEG activity in consecutive 30 s epochs. More recent studies have been introduced in sleep research based on the nature and quantitation of the sleep *microstructure*, taking into account the time structure of phasic EEG events observed during non-REM (NREM) stage and shorter than the standardized scoring epoch.

The detection of these events is a fundamental tool for the identification of the Cyclic Alternating Pattern (CAP), which is characterized by sequences of transient EEG variations (phase A) breaking away from the background rhythm of the ongoing sleep stage. Each phase A is characterized by an abrupt frequency/amplitude shift, which coincides with a higher level of brain activation and recurs at intervals up to 1 min long. The intermittent recovery of background activity identifies the interval (phase B) that separates the phases A and corresponds to a lower level of activation. Both A and B phases can last between 2 and 60 s. A CAP cycle is composed of a phase A, and the following phase B. At least two

* Corresponding author. Address: Politecnico di Milano, Department of Biomedical Engineering, via Golgi 39, 20133 Milan, Italy. Tel.: +39 02 2399 9503; fax: +39 02 2399 9508.
E-mail address: sara1.mariani@mail.polimi.it (S. Mariani).

1388-2457/$36.00 © 2011 International Federation of Clinical Neurophysiology. Published by Elsevier Ireland Ltd. All rights reserved.
doi:10.1016/j.clinph.2011.02.031

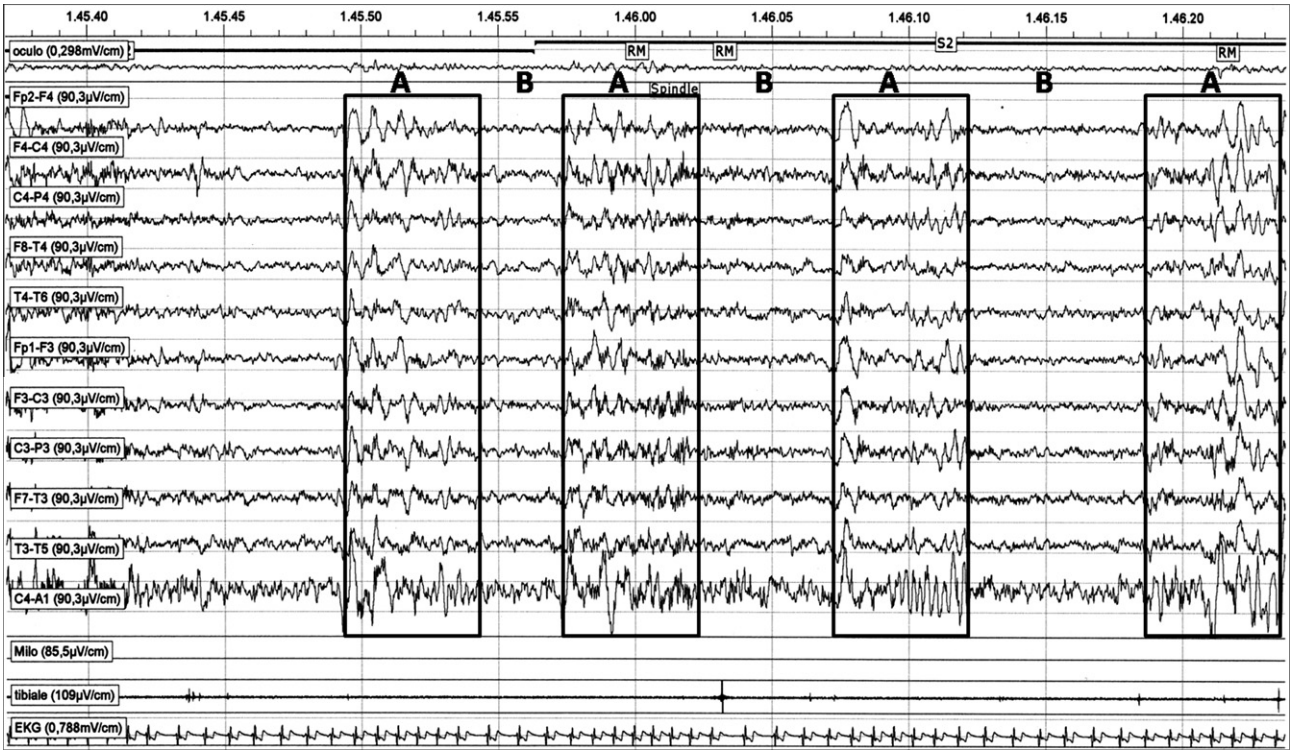

Fig. 1. An example of CAP sequence in sleep stage 2. The boxes outline the phases A of CAP. The EOG, 11 EEG leads, the EMG and the EKG are shown in the screenshot.

consecutive CAP cycles are needed to define a CAP sequence, as shown in Fig. 1. The remaining NREM sleep not occupied by CAP sequences is scored as non-CAP (NCAP).

In relation to the EEG features that compose the phase A of CAP, spectral contents allow classification of three subtypes: (a) A1, dominated by high-voltage delta waves (0.5–4 Hz); (b) A2, when rapid activities occur for 20–50% of the total activation time; (c) A3, characterized by rapid activities, especially beta (15–30 Hz), that occupy more than the 50% of the total phase A duration (Terzano and Parrino, 2000).

In the dynamic organization of sleep, CAP expresses a condition of instability of the level of vigilance that translates the brain effort to preserve and regulate sleep macrostructure. In particular, subtypes A1 are mostly involved in the build-up and consolidation of slow-wave sleep, while subtypes A2 and A3 are closely related and modulate the onset of REM sleep (Terzano et al., 2005).

Specific alterations of phase A subtypes have been described in a number of sleep disorders such as nocturnal frontal lobe epilepsy (Zucconi et al., 2000), sleep apnea (Terzano et al., 1996), insomnia (Terzano et al., 2003; Parrino et al., 2004) and narcolepsy (Terzano et al., 2006).

At the present time, analysis of CAP parameters is performed only through visual methods by identifying EEG events such as delta bursts, vertex sharp transients, K-complex sequences with or without spindles, polyphasic bursts, K-alpha, intermittent alpha, EEG arousals, which constitute the basic phase A features for CAP scoring (Terzano et al., 2001).

In spite of the consolidated relevance of the visual methodology, still the gold standard for scoring sleep, the quantitative assessment of sleep measures is a time-consuming procedure. Moreover, visual analysis can be biased by a certain degree of inter-scorer agreement, ranging from 69% to 77% (Rosa et al., 2006). In order to overcome these issues, the research of quantitative measures of the EEG, capable of distinguishing CAP A phases from the background, is desirable with the final purpose of achieving an automatic detection algorithm. So far, only a few studies have presented methods for the automatic analysis of CAP (Rosa et al., 1999; Navona et al., 2002; Barcaro et al., 2004; De Carli et al., 2004; Largo et al., 2005; Ferri et al., 2005).

In all these methods, the computation of "short–long term ratios", performed in combination with other methods of analysis and often connected to a model for the sleep EEG generation, has allowed the achievement of interesting results. However, a robust universal method for the detection of CAP is still missing and nowadays it is not easy to introduce CAP studies in everyday clinics with appropriate confidence and fast scoring.

The aim of this work is to exploit the results of previous studies, integrated by an analytical evaluation of the information content of each descriptor and introducing new descriptors that could improve the automatic recognition of CAP A phases.

2. Methods

The data analyzed in this study were extracted from all-night PSG recordings collected at the Parma Sleep Disorders Centre database. Eight normal subjects, four males and four females, aged between 23 and 35 years (23-year-old subjects, one 24, two 30-year-old, one 31, one 32 and one 35), were selected after the accomplishment of an entrance investigation. Subjects were evaluated in order to obtain a homogeneous group and were free from psychiatric, neurological and medical disorders. Sleep/wake schedule was investigated for 14 days before the PSG recordings with a sleep log. Inclusive criteria were the absence of sleep disorders and daytime napping. A personal interview integrated by a structured questionnaire confirmed good vigilance level during daytime, normal sleep habits without any difficulties in falling or remaining asleep at night. All participants were requested to refrain from any drug intake and excessive alcohol or coffee consumption in the previous 3 weeks preceding the PSG recording. All subjects slept at least two consecutive nights in a video-monitored, temperature-controlled and sound-proof (Leq < 35 dB) laboratory. The first night was used for adaptation to the recording

Table 1
Dataset used for the analysis: for each subject, the total polysomnography time, the total NREM time, and the total time corresponding to CAP A phases are reported.

Subject	Total sleep time (s)	NREM time (s)	A phase time (s)
1	30,780	22,044	4703
2	31,200	21,273	4257
3	29,539	19,800	3113
4	30,030	20,077	3024
5	30,840	20,280	1935
6	29,040	19,290	3427
7	29,690	19,710	2132
8	29,310	22,170	3714
	240,429	**164,644**	**26,305**

environment and for screening respiratory or other sleep-related disorders. Exclusion criteria were: apnea-hypopnea index $\geqslant 5$ and/or PLM index $\geqslant 15$, in order to avoid an increase of CAP rate, alterations of phase A subtypes distribution and CAP sequences duration, induced by apnea or periodic limb movements. The polysomnographic recordings lasted around 8 h each, and included several EEG derivations, the electromyogram (EMG) and the electrocardiogram (ECG). Each signal was recorded and examined by an expert clinician.

The expert visually scored the following events following the respective guidelines (Rechtschaffen and Kales, 1968), (Terzano et al., 2001):

- Sleep macrostructure: sleep stages 1–4, wake, REM sleep, movement artifacts.
- Sleep microstructure: activations (A-phase candidates) and their subtypes: A1, A2 or A3.

The EEG C3-A2 or the C4-A1 traces were equivalently used for the data analysis. The traces were sampled at a frequency equal to 100 Hz. The segments relative to wake and REM sleep were removed, leaving the analysis only to NREM sleep. This lead to the final dataset reported in Table 1.

2.1. Band descriptors

The remaining EEG signal was first filtered with a low-pass anti-aliasing filter at 30 Hz. Then, it was separated in the six bands commonly used in clinics: $0.5 < \text{low delta} \leqslant 2$ Hz, $2 \text{ Hz} < \text{high delta} \leqslant 4$ Hz, $4 < \text{theta} \leqslant 8$ Hz, $8 \text{ Hz} < \text{alpha} \leqslant 12$ Hz, $12 < \text{sigma} < 15$ Hz, $15 \leqslant \text{beta} < 30$ Hz. A FIR filter with 30 coefficients and a Kaiser window was used for this purpose. For each time series $x(n)$ where n is the considered sample, filtered in a specific band b i.e., $x_b(n)$, the resulting signal was squared and normalized between 0 and 1 (with respect to the maximum power in the band), and finally averaged over non-overlapped time windows of length equal to 1 s, leading to the instantaneous power time series (Pfurtscheller and Lopes da Silva, 1999) $x^2_{\text{bn}}(t)$, where t is the second of interest, and for each $x^2_{\text{bn}}(t)$, two types of descriptors were computed:

$$d_{\text{b1}}(t) = \frac{x^2_{\text{bn}}(t)}{p_{\text{e}}} \tag{1}$$

$$d_{\text{b2}}(t) = \frac{p_{\text{s}}(t) - p_{\text{l}}(t)}{p_{\text{l}}(t)} \tag{2}$$

where $x^2_{\text{bn}}(t)$ is the normalized power in the considered band b at each second t, p_{e} is its mean value during the considered sleep stage, as scored by the physician, and p_{s} and p_{l} are the mean power in the considered band computed on a window of 2 and 64 s, respectively, centered on the second t of interest. The need to normalize the instantaneous power with respect to the mean power over a longer time interval reflects the idea to highlight the transient frequency/amplitude variations of the order of 2–60 s that are typical of CAP and are outlined against the background, that can vary significantly from one sleep stage to another.

Even after the filtering and the averaging steps required for the computation of the descriptors, some outlier values remained, due to electrical or movement artifacts. These values were removed before normalization as follows: the mean value and the standard deviation (σ) were computed for each descriptor, and values that exceeded a threshold equal to 10σ were set to zero. This threshold was selected empirically by a visual inspection of some signal seg-

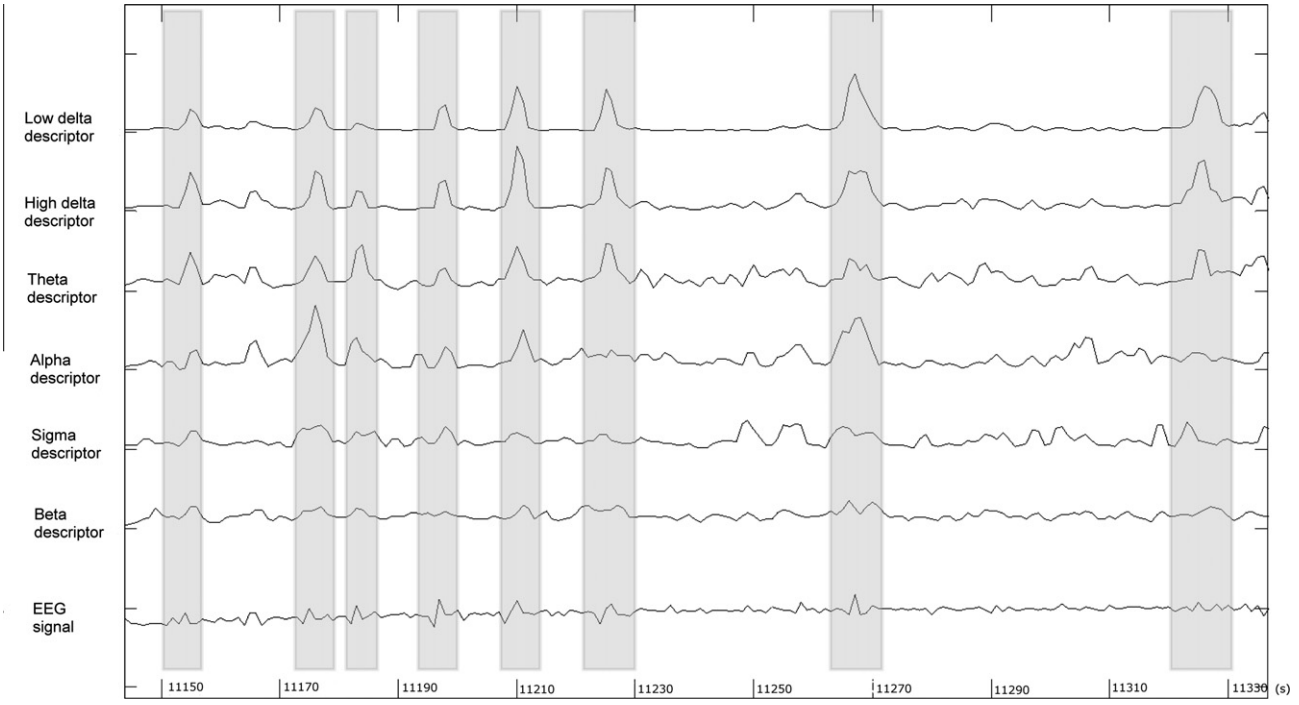

Fig. 2. Behavior of the band descriptors (computed according to descriptor type d_{b2}) in correspondence with the visually scored activations. The transparent bars show the borders of the activations.

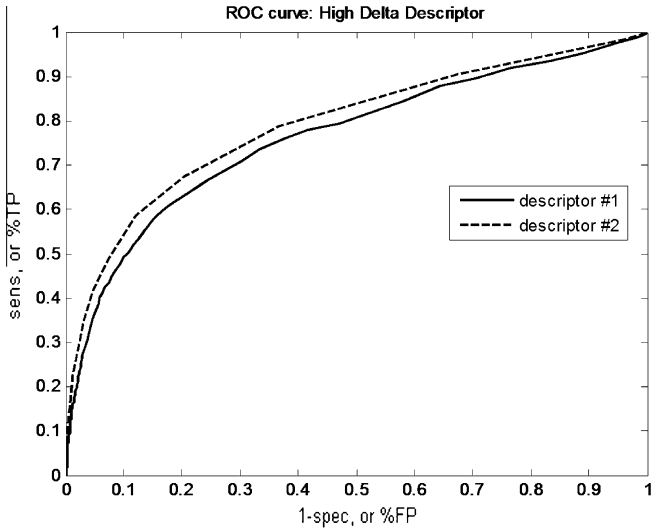

Fig. 3. ROC curves for the two different high delta descriptor types (1) and (2): the solid curve represents descriptor type (1), the dashed curve descriptor type (2).

ments extracted from different subjects where the expert physician had recognized movement artifacts, and was chosen according to a trade-off between artifact removal and preservation of the signal of interest. The descriptors were normalized again between 0 and 1 with respect to their maximum value.

Fig. 2 shows an example of the trend of the six band descriptors obtained with the technique (2) in correspondence of the visually recognized phases A during sleep stage 2: it can be noticed that all the descriptors, especially those in the low frequency bands, have a certain amplitude increase in correspondence of the visually-scored phases A.

The potential activations were detected by superimposing a threshold (the threshold value varying between 0 and 1 in steps of 0.005) for all the subjects, band descriptors, and descriptor types and considering as belonging to A phases the 1 s intervals where the descriptors overcome the threshold, while considering as belonging to the background all the other intervals.

The visual scoring provided by the expert neurophysiologist, used as the golden standard, and the results obtained by the linear separation were compared through the ROC curves. Fig. 3 shows the results for the high delta descriptor computed with the two different descriptor types d_{b1} and d_{b2}: the solid line represents the ROC curve obtained with d_{b1}, while the dashed line represents the ROC curve obtained with d_{b2}.

Since $d_{b1}$and d_{b2} showed similar performances in all situations, the second descriptor type was chosen because its computation does not require the scoring of the macrostructure, except for the mere wake/NREM/REM distinction, making it more suitable for a completely automatic detection algorithm.

The ROC curves for each band descriptor were computed with technique (2) in order to quantitatively analyze the relevance of the band descriptors in distinguishing the activations from the non-activations.

The recognition statistics sensitivity, specificity, and accuracy were computed in the following way: for each band descriptor the data from the whole eight subjects dataset were merged and the ROC curves calculated. The optimal threshold was selected as the one in correspondence of which the ROC curve was closest to the perfect classification point (0,1).

2.2. Hjorth descriptors in the low delta and high delta bands

A further study was conducted over the Hjorth parameters (Hjorth, 1970) applied to the high delta and to the low delta bands. We concentrated on these two bands since they demonstrated to be the most promising in characterizing A phases of CAP (see Fig. 2 and the results from Section 3.1.). The first Hjorth parameter is called *activity* and it is simply the variance σ^2 of the signal segment. A second parameter, called *mobility* M_x, is computed as the square root of the ratio between the activity of the first derivative of the signal and the activity of the (original) signal:

$$M_x = \left[\frac{\sigma_{x'}^2}{\sigma_x^2}\right]^{\frac{1}{2}} = \frac{\sigma_{x'}}{\sigma_x} \tag{3}$$

where x' stands for the first derivative of the signal. Thus, mobility represents the variance of the slopes normalized by the variance of the amplitude distribution of the time series. In the frequency domain, mobility can be interpreted as the standard deviation of the power spectrum. High values of M_x are obtained for spectra with a high fraction of fast activity. A third parameter, called *complexity* C_x, or the *form factor FF*, is defined as the ratio between the mobility of the first derivative of the signal and the mobility of the signal itself:

$$C_x = \frac{M_{x'}}{M_x} = \frac{\sigma_{x''}/\sigma_{x'}}{\sigma_{x'}/\sigma_x} \tag{4}$$

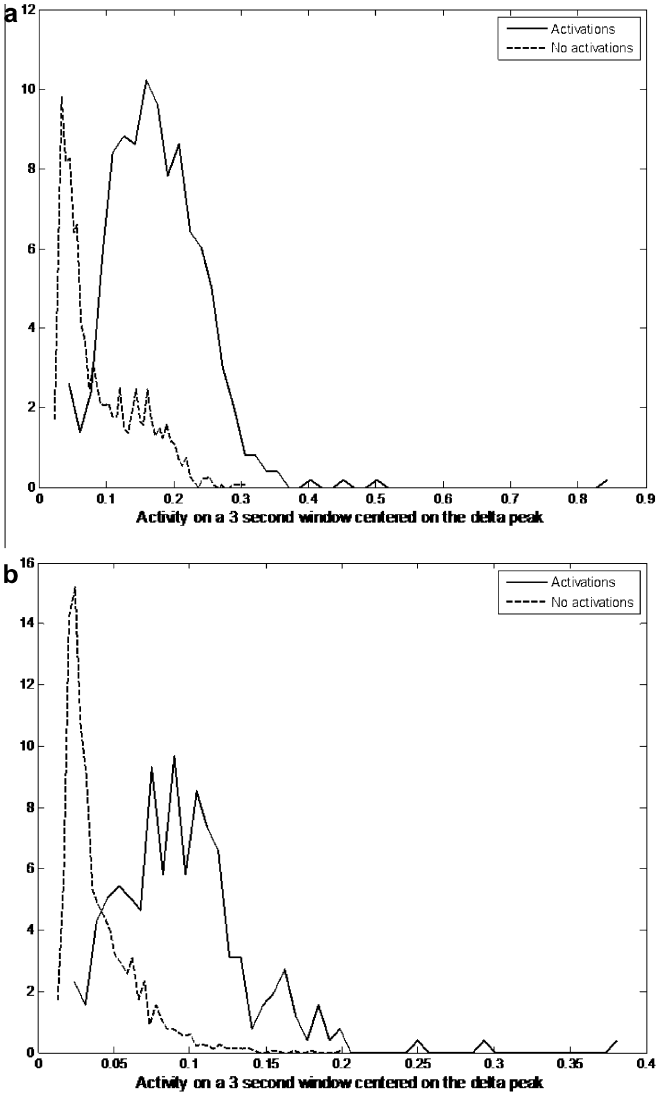

Fig. 4. (a) Distribution of the activity in the low delta band after a first automatic detection through the thresholding on the low delta descriptor, (b) distribution of the activity in the high delta band after a first automatic detection through the thresholding on the high delta descriptor.

where x'' is the second derivative of the signal. The complexity of a sinusoidal wave is unity, other waveforms have complexity values increasing with the extent of variations present in them. The idea was to use these parameters to capture the overall increase of the delta power occurring during the activations over a long time span, in order to avoid misclassification due to spurious peaks in the low delta and high delta descriptors not belonging to activations.

As a first step for the evaluation of these parameters, a low threshold, equal to 0.04, selected to allow for a high sensitivity, was applied to the low and high delta descriptors to find some candidate segments. For each candidate, the average activity, mobility and complexity in the low delta and high delta band, respectively, were computed over 3 s windows centered on the first second where the threshold was passed. Dealing with sampled data, derivatives were approximated by computing the incremental ratio of the vectors.

This was done for two classes of automatically scored activations: true and false positives. The histograms of the three Hjorth parameters were plotted for the two classes. While the parameters mobility and complexity could not separate the two classes of data, the histograms for the activity are quite distinct, and are shown in Fig. 4. It was thus concluded that the introduction of two new descriptors, based on the Hjorth activity calculated on the EEG signal filtered in the low delta and the high delta bands on overlapped 3 s windows would add information to that provided by the low delta and high delta band descriptors.

These descriptors were thus added to the previous, and the ROC curves and the recognition statistics were computed similarly to what was done for the band descriptors.

2.3. Differential variance of the EEG signal

The variance of the raw EEG signal in non-overlapping windows of 1 s was obtained. The variance difference between one 1 s window and the previous one was calculated and the result normalized by its maximum value. Outliers were eliminated from the raw EEG signal with the same process defined in Section 2.1. Fig. 5 shows a typical example of the change in EEG variance together with the visually detected activations during sleep stage 2. The information content for this feature was evaluated by means of the ROC curves like for the other features.

2.4. Information content and elimination of the redundancy

As a final step, we wanted to identify any redundant information among the nine descriptors listed above (six band descriptors, the activity in the low delta and in the high delta bands, and the EEG differential variance). In fact, redundancies in the features could not only enlarge the computational burden for a future implementation of a classifier, but also introduce noise in the classification. In order to do so, the Pearson's product-moment correlation coefficient was computed between each possible couple of descriptors (Boslaugh and Watters, 2008).

Furthermore, Principal Component Analysis (PCA) was carried out over the nine descriptors with the purpose to reduce the feature space dimensionality. PCA is a statistical technique to reduce dataset dimensionality by removing features that are linear combination of others. It consists of an orthogonal linear transformation that projects the data onto a new coordinate system such that the greatest variance of any projection of the data comes to lie on the first coordinate (called the first principal component), the second greatest variance on the second coordinate, and so on. Once the patterns in the data have been found, it allows compressing the data without much loss of information by simply selecting a certain number of coordinates (principal components) that, combined, contain a significant portion of the information of the whole dataset (Smith, 2002).

An analysis of the information content of the principal components was carried out by using one component at the time to per-

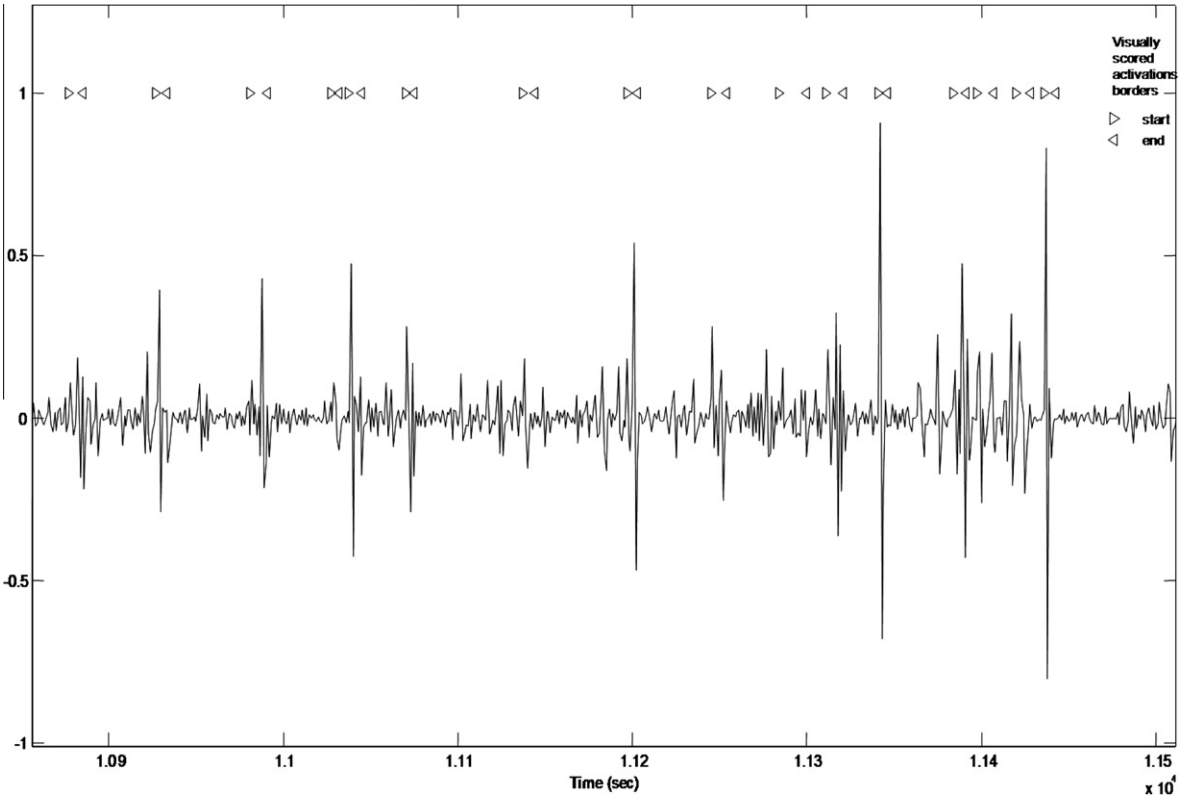

Fig. 5. Peaks of the differential variance in correspondence of the visually scored A-phases.

form a classification of CAP A phases by threshold similarly to what was done for the descriptors: the optimal threshold, i.e. the one for which the ROC curves were closest to the perfect classification point (0,1) was determined over the eight subjects dataset and, for that threshold value, the statistics sensitivity, specificity and accuracy were computed.

3. Results

3.1. Band descriptors

We report as an example the ROC curves calculated with one subject's data for every descriptor in Fig. 6.

All the ROC curves are very different from the bisector of the first quadrant, and those relative to the low delta and high delta descriptors are the closest to the perfect classification point (0,1).

We report in Table 2 the values of sensitivity, specificity and accuracy of the classification on the whole dataset obtained for each descriptor. The optimal thresholds are also reported in the table.

3.2. Activity in the low delta and high delta bands

A ROC curve for the low delta activity and one for the high delta activity are reported in Fig. 7.

Here, it can also be noticed how both curves get very close to the perfect recognition point (0,1). The statistics obtained on the whole dataset, by using the optimal group thresholds are shown in Table 3.

3.3. Differential variance of the EEG signal

A ROC curve for the differential variance of the raw EEG signal, obtained computing the absolute value of the descriptor and applying a threshold similarly as for the previous descriptors, is reported in Fig. 8.

The statistics on the eight subjects, obtained with the optimal threshold value, are shown in Table 4 and indicate that this descriptor is also capable of obtaining a good accuracy value in the recognition of A phases, equal to 72.44, even if used alone.

3.4. Information content and elimination of the redundancy

The correlation coefficients are reported in Table 5.

The descriptors mostly show complementary information content, as can be inferred from the correlation coefficients, which

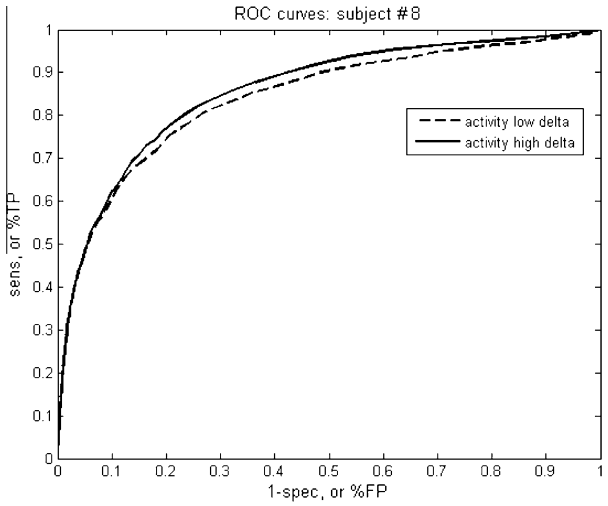

Fig. 7. ROC curves for the activity in the low delta and in the high delta bands.

Table 2
Detection statistics obtained on the whole dataset using each band descriptor and the optimal thresholds.

	Low delta	High delta	Theta	Alpha	Sigma	Beta
Mean sensitivity (%)	58.59	59.00	61.15	59.86	64.80	53.48
Mean specificity (%)	70.66	71.13	67.51	65.27	58.96	64.82
Mean accuracy (%)	68.73	69.19	66.49	64.41	59.90	63.01
Optimal threshold	0.08	0.12	0.165	0.14	0.11	0.168

Table 3
Detection statistics obtained on the whole dataset, using the low delta activity and the high delta activity and the optimal thresholds.

	Low delta activity	High delta activity
Mean sensitivity (%)	71.70	69.59
Mean specificity (%)	70.56	71.90
Mean accuracy (%)	70.74	71.53
Optimal threshold	0.11	0.20

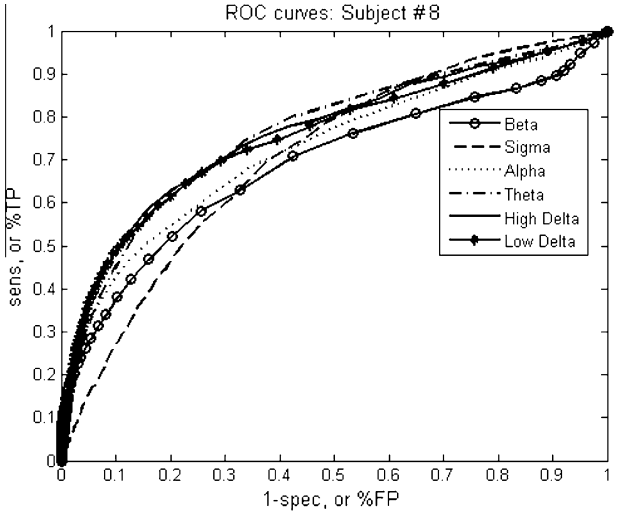

Fig. 6. ROC curves for subject number eight and for every band descriptor.

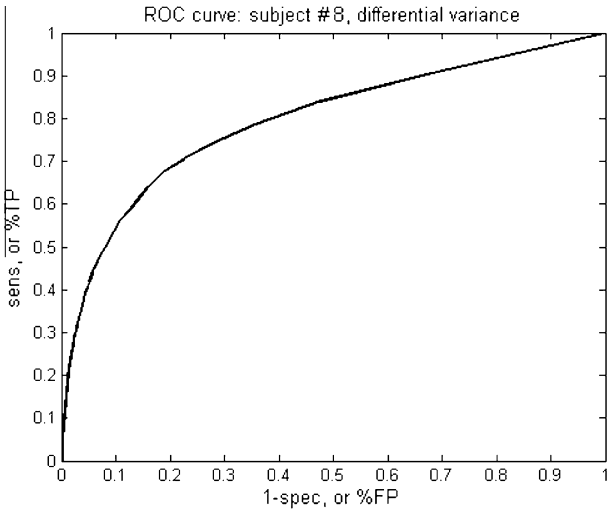

Fig. 8. ROC curves for the differential EEG variance.

are, in general, indicative of a moderate or low linear dependence. The only exceptions are those of the low delta and high delta descriptors, having a correlation coefficient equal to 0.86, and the low delta and high delta Hjorth activity, having a correlation coefficient equal to 0.92. Therefore, in the light of an automatic classification, in order to avoid redundant information and lighten the computational burden, the low delta descriptor and the low delta activity could be eliminated in favor of those in the high delta band, having a higher accuracy and containing about the same information or, in alternative, a single band descriptor and a single activity descriptor could be used for the whole delta band (0.5 – 4 Hz).

Table 4
Detection statistics obtained on the whole dataset using the differential variance of the EEG, and the optimal threshold.

	Differential variance
Mean sensitivity (%)	51.59
Mean specificity (%)	76.40
Mean accuracy (%)	72.44
Optimal threshold	0.02

Table 5
Correlation coefficients for every descriptor with one another. Due to its symmetry, only half of the table is shown.

	Low δ	High δ	θ	α	σ	β	Low δ act	High δ act	Var.
Low δ	1	0.86	0.59	0.37	0.29	0.26	0.47	0.46	0.29
High δ		1	0.72	0.42	0.32	0.28	0.46	0.52	0.31
θ			1	0.53	0.36	0.35	0.35	0.42	0.24
α				1	0.46	0.46	0.23	0.25	0.15
σ					1	0.59	0.20	0.21	0.13
β						1	0.14	0.11	0.10
Low δ act							1	0.92	0.53
High δ act								1	0.55
Var									1

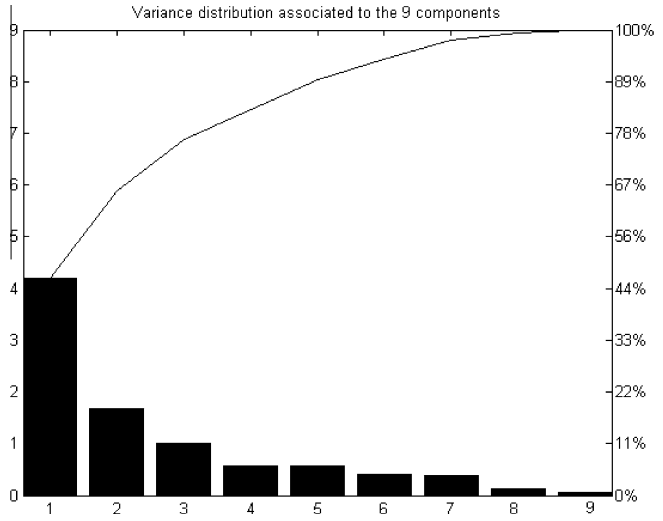

Fig. 9. The histogram shows the variance distribution (or information content) associated to the nine components. The curve shows its cumulative sum.

At the same time, the information content for the first nine principal components, obtained thanks to the PCA, is exemplified in the histogram in Fig. 9. The first six principal components contain the 94% of the information, while the first seven components contain the 98%. Table 6 shows the principal components coefficients, or loadings. It is a p-by-p matrix, each column containing coefficients for one principal component. The columns are in order of decreasing component variance. Finally, the results of the classification performed by employing one principal component at the time are shown in Table 7. The statistics sensitivity, specificity and accuracy obtained by using the optimal threshold are reported.

The data can thus be projected onto the space of the first six or seven principal components, and the new dataset can be used for the automatic analysis. Therefore, the computational cost for the classification could be reduced by using only the six or seven components for the development of an automatic detection method.

4. Discussion

This study provides objective characterization of sleep microstructure, attributing a statistical value to the spectral components of CAP. Although it was performed on a sample of only eight subjects, approximately 8 h of sleep were used for each subject, and the analysis was performed on descriptors calculated on 1 s long windows, leading to a total dataset of 59,673 samples for each descriptor, 27,284 of those belonging to visually scored phases A of CAP. This dataset can be considered large enough to allow for a significant characterization of A phases. A clinical validation should however be performed on a larger number of subjects after employing the analyzed features for training an automatic classifier.

The current results show that it is possible to extract *quantitative* and not only qualitative parameters that characterize CAP A phases and exploit them for automatic recognition. This confirms that CAP is not a mere visual artifact, but finds objective evidence in the non-conventional, mathematical approach. So far, the study of CAP sleep has been criticized because of its "man-conditioned" nature: its identification is strictly linked to the expertise of the observer, and thus a certain hesitation has been encountered for its implementation on a large scale. This study, attributing a quantitative value to the information content of descriptors extracted from

Table 6
PCA loadings: each column reports the weights by which each descriptor is weighted to obtain the corresponding principal component. The columns are in order of decreasing component variance.

	Principal components								
	1	2	3	4	5	6	7	8	9
Low_delta	0.3868	−0.0114	0.4316	−0.3130	0.1446	0.0167	0.4514	−0.5051	−0.2931
High_delta	0.4106	0.0071	0.4371	−0.1781	0.1194	0.0240	0.0589	0.6914	0.3349
Theta	0.3759	0.1521	0.3142	0.2711	0.0170	−0.0199	−0.7616	−0.2874	−0.0073
Alpha	0.2985	0.3551	−0.0619	0.7432	−0.1880	0.0265	0.4369	0.0410	0.0062
Sigma	0.2621	0.4182	−0.3888	−0.3315	−0.0676	0.6957	−0.0803	−0.0133	0.0166
Beta	0.2374	0.4713	−0.3687	−0.2733	0.1428	−0.6969	−0.0320	0.0416	−0.0463
Activity_low_delta	0.3541	−0.4037	−0.2522	−0.0894	−0.3946	−0.1261	0.0598	−0.2991	0.6127
Activity_high_delta	0.3669	−0.4035	−0.2057	−0.0128	−0.3648	−0.0428	−0.1034	0.3015	−0.6508
Variance	0.2577	−0.3576	−0.3566	0.2273	0.7845	0.1035	0.0099	−0.0150	0.0202

Table 7
Detection statistics obtained on the whole dataset using one principal component at the time.

	1	2	3	4	5	6	7	8	9
Mean sensitivity (%)	70.84	35.00	32.52	51.71	42.55	45.21	43.35	40.01	35.57
Mean specificity (%)	74.57	61.96	61.30	60.46	67.55	58.27	64.38	67.68	65.72
Mean accuracy (%)	73.98	57.65	56.71	59.07	63.55	56.18	61.02	63.26	60.90

the EEG, and showing that this information content is generally significant in characterizing the A phases, gives a foundation of mathematical objectivity to what is seen by the human eye.

The Hjorth parameters, employed in this study, have already been used for the evaluation of sleep quality in rats in 1993 (Depoortere et al., 1993). Activity, mobility, and complexity were calculated from rat EEG to automatically recognize sleep stages in rats. In particular, the activity distribution over the total recording permitted the evaluation of the quality of sleep, especially by examining the index and rate of unstable amplitude segments (UAS), that constitute in rats the equivalent of CAP in humans.

The ROC curves show how all the identified features have some information content in characterizing CAP A phases, since they show significant difference from the bisector of the first quadrant. In particular, the delta descriptor and the delta activity play the main role, having the highest accuracy in distinguishing the A phases from the background. The value of the delta power is extremely important, since it remarks the role of A1-subtype, which represent, in physiological conditions, over 50% of all A phases, and constitutes a means of partial brain activation while preserving the continuity of sleep.

In spite of the relevant information content, no single descriptor provides a sufficient accuracy in recognizing the A phases by itself; however, the differential variance presents similar separation performance when compared to previous works (Navona et al., 2002). Even applying the PCA and extracting the first principal component, that would only contain the 44% of the information. Therefore, no sole parameter, in the original space or in the principal component space, can be used by itself: we expect an automatic analysis to be valid only if it is based on the integration of more than one feature. This is due to the great complexity of CAP and finds an explanation in the wide atlas of rules that have to be followed in the visual analysis and in the variety of A phase subtypes.

This study demonstrates once again how CAP is a complex EEG phenomenon, and how a skillful expertise of sleep EEG is mandatory to score CAP. Therefore, since the automatic method only remarks the value of a human intuition, the analysis of CAP is a demanding challenge even in the most expert hands. There is a need of instruments that, if properly used, make the quantitation of the traces handier and reduce to the minimum the inter-scorer variability. In this direction, sleep experts have formulated possible solutions. Several studies have extracted EEG features and computed band descriptors for the automatic detection of CAP A-phases (Rosa et al., 1999; Navona et al., 2002; Barcaro et al., 2004; De Carli et al., 2004; Largo et al., 2005 and Ferri et al., 2005). These authors computed some sort of band descriptors based on short-long term ratios, and obtained good accuracy results when implementing the automatic methods. However, most methods examined a chosen selection of CAP A phases, or required the assistance of a sleep expert during the automatic recognition process. This study exploited similar band descriptors, but also introduced new descriptors based on Hjorth activity to account for the variation in the delta band amplitude (intermittent delta) and based on the EEG variance to account for the abrupt frequency variations occurring during the beginning and end of A phases. It must be kept in mind the difference between the ideal laboratory environment, where the studies come from a selection of A phases, and the use in clinical practice, where the signals are subject to noise and artifacts. This study rises from an increasing need for an instrument to study sleep stability, that is an important value for sleep quality, together with duration, depth, and continuity of sleep (De Carli et al., 2004; Parrino et al., 2004).

It must be remarked that this study implemented a general analysis of the characteristics of the A phases of CAP without distinguishing among the three A phase subtypes. In fact, we wished to quantitatively examine the spectral content of all A phases without any bias on their subtype. The high significance of the delta descriptor and the delta activity in representing the A phases meets its response not only in the usual presence of an initial delta peak in all A phases, but also in the prevalence of A1 subtype A phases during sleep (Terzano and Parrino, 2000) demonstrated that A1 subtype represents the 90% of A phases in the construction of deep sleep and the 65% in its destruction, while (Smerieri et al., 2007) showed that phase A1 subtypes prevail in all CAP sequences.

The statistical relevance of high and low delta rhythms, that dominate in subtypes A1, is quantified here in its main role as a marker for distinguishing A phases. Furthermore, the variability (activity) of the delta rhythm is important as an expression of A1 phases, and this finds an important statistical confirmation in the results of this study.

Besides creating the premises for a future tool for the automatic analysis of CAP sleep, this study provides a quantitative measure of the value of slow-wave activity (see activity descriptor), laying the bases for future investigation on the involvement of subtype A1 in neuropsychological processes. Sleep slow-wave activity (frequency range between 0.5 and 4 Hz) has already been indicated as a significant marker of learning consolidation during sleep (Ferri et al., 2008), and a quantitative analysis has confirmed that CAP A1 subtypes are associated with higher cognitive functioning, whereas A3 subtypes are associated with lower cognitive functioning (Ferri et al., 2010). These premises reinforce the role of CAP investigation in sleep studies and enhance the importance of reliable automatic procedures.

Acknowledgement

This work was supported in part by PSYCHE under Project FP7-247777 of the European Community.

References

Barcaro U, Bonanni E, Maestri M, Murri L, Parrino L, Terzano MG. A general automatic method for the analysis of NREM sleep microstructure. Sleep Med. 2004;5:567–76.

Boslaugh S, Watters DPA. Statistics in a nutshell. Sebastopol, CA, USA: O'Reilly & Associates, Inc.; 2008.

De Carli F, Nobili L, Beelke M, Watanabe T, Smerieri A, Parrino L, et al. Quantitative analysis of sleep EEG microstructure in the time-frequency domain. Brain Res. Bull. 2004;63:399–405.

Depoortere H, Francon D, Granger P, Terzano MG. Evaluation of the stability and quality of sleep using hjorth's descriptors. Physiol. Behav. 1993;54:785–93.

Ferri R, Bruni O, Miano S, Smerieri A, Spruyt K, Terzano MG. Inter-rater reliability of sleep cyclic alternating pattern (CAP) scoring and validation of a new computer-assisted CAP scoring method. Clin. Neurophysiol. 2005;116:696–707.

Ferri R, Drago V, Aricò D, Bruni O, Remington RW, Stamatakis K, et al. The effects of experimental sleep fragmentation on cognitive processing. Sleep Med. 2010;11:378–85.

Ferri R, Huber R, Aricò D, Drago V, Rundo F, Ghilardi MF, et al. The slow-wave components of the cyclic alternating pattern (CAP) have a role in sleep-related learning processes. Neurosci. Lett. 2008;432:228–31.

Hjorth B. EEG analysis based on time domain properties. Electroencephalogr. Clin. Neurophysiol. 1970;29:306–10.
Largo R, Munteanu C, Rosa A. CAP event detection by wavelets and GA tuning. IEEE International Workshop on Intelligent Signal Processing – Proceedings 2005:44–48.
Navona C, Barcaro U, Bonanni E, Di Martino F, Maestri M, Murri L. An automatic method for the recognition and classification of the A-phases of the cyclic alternating pattern. Clin. Neurophysiol. 2002;113:1826–31.
Parrino L, Ferrillo F, Smerieri A, Spaggiari MC, Palomba V, Rossi M, et al. Is insomnia a neurophysiological disorder? The role of sleep EEG microstructure. Brain Res. Bull. 2004;63:377–83.
Pfurtscheller G, Lopes da Silva FH. Event-related EEG/MEG synchronization and desynchronization: basic principles. Clin. Neurophysiol. 1999;110:1842–57.
Rechtschaffen A, Kales A. A manual of standardized terminology, techniques and scoring system for sleep stages in human subjects. National Institutes of Health Publications; 1968. p. 204.
Rosa A, Alves GR, Brito M, Lopes MC, Tufik S. Visual and automatic cyclic alternating pattern (CAP) scoring: inter-rater reliability study. Arq. Neuropsiquiatr. 2006:64.
Rosa AC, Parrino L, Terzano MG. Automatic detection of cyclic alternating pattern (CAP) sequences in sleep: preliminary results. Clin. Neurophysiol. 1999;110:585–92.
Smerieri A, Parrino L, Agosti M, Ferri R, Terzano M. Cyclic alternating pattern sequences and non-cyclic alternating pattern periods in human sleep. Clin. Neurophysiol. 2007;118:2305–13.
Smith LI. A Tutorial on Principal Components Analysis 2002, vol. 51. Cornell University: USA; 2002. p. 52.
Terzano MG, Parrino L, Boselli M, Spaggiari MC, Di Giovanni G. Polysomnographic analysis of arousal responses in obstructive sleep apnea syndrome by means of the cyclic alternating pattern. J. Clin. Neurophysiol. 1996;13:145–55.
Terzano MG, Parrino L, Sherieri A, Chervin R, Chokroverty S, Guilleminault C, et al. Atlas, rules, and recording techniques for the scoring of cyclic alternating pattern (CAP) in human sleep. Sleep Med. 2001;2:537–53.
Terzano MG, Parrino L, Spaggiari MC, Palomba V, Rossi M, Smerieri A. CAP variables and arousals as sleep electroencephalogram markers for primary insomnia. Clin. Neurophysiol. 2003;114:1715–23.
Terzano MG, Parrino L. Origin and significance of the Cyclic Alternating Pattern (CAP): review article. Sleep Med. Rev. 2000;4:101–23.
Terzano M, Parrino L, Smerieri A, Carli F, Nobili L, Donadio S, et al. CAP and arousals are involved in the homeostatic and ultradian sleep processes. J. Sleep Res. 2005;14:359–68.
Terzano M, Smerieri A, Del Felice A, Giglia F, Palomba V, Parrino L. Cyclic alternating pattern (CAP) alterations in narcolepsy. Sleep Med. 2006;7:619–26.
Zucconi M, Oldani A, Smirne S, Ferini-Strambi L. The macrostructure and microstructure of sleep in patients with autosomal dominant nocturnal frontal lobe epilepsy. J. Clin. Neurophysiol. 2000;17:77–86.